Zeitschrift für Kristallographie 213, 123–129

Single crystal structure determination of cetylpyridiniumammonium bromide and Rietveld structure determination of cetylquinuclidinium bromide

P. Ballirano*

Corso Duca di Genova 147, I-00121 Roma, Italy

R. Caminiti, C. Sadun

Università di Roma "La Sapienza", Istituto Nazionale per la Fisica della Materia, P.le A. Moro 5, I-00185 Roma, Italy

V. M. Coiro

Area di Ricerca del CNR, Istituto di Strutturistica Chimica "G. Giacomello", C.P. 10, I-00016 Monterotondo St., Roma, Italy

G. Mancini

Università di Roma "La Sapienza", Centro CNR di Studio sui Meccanismi di Reazione, Dipartimento di Chimica, P.le A. Moro 5, I-00185 Roma, Italy

and A. Maras

Università di Roma "La Sapienza", Dipartimento di Scienze della Terra, P.le A. Moro 5, I-00185 Roma, Italy

Received May 5, 1997; accepted in final form August 16, 1997

Abstract. The structures of cetylpyridiniumammonium bromide (CPyB) and cetylquinuclidinium bromide (CQB), two tetraalkylammonium bromide surfactants, are reported. In particular, whereas the structure solution of CPyB was carried out through conventional single-crystal diffractometry, the structure of CQB has been determined by means of powder diffractometry. CPyB crystallizes in $P\bar{1}$ space group with cell parameters $a = 7.618(2)$ Å, $b = 5.554(1)$ Å, $c = 27.474(7)$ Å, $\alpha = 95.03(2)°$, $\beta = 95.65(2)°$, $\gamma = 100.89(2)°$, $V = 1129.2(5)$ Å^3 ($R = 0.066$, $wR = 0.054$): CQB also in $P\bar{1}$ with cell parameters $a = 8.1395(8)$ Å, $b = 6.4475(7)$ Å, $c = 25.237(2)$ Å, $\alpha = 99.921(6)°$, $\beta = 93.123(9)°$, $\gamma = 111.956(9)°$, $V = 1222.9(2)$ Å^3 ($R_p = 0.097$, $wR_p = 0.128$, $R_{exp} = 0.078$, and $R(F^2) = 0.127$).

Introduction

Tetraalkylammonium bromide surfactants are widely used as catalysts in micellar chemistry [1]. In general the X-ray structure solution of the surfactants used in organic reactions may contribute to further understanding what can be observed by reactivity, and could help in addressing the choice of the best surfactant to achieve chemio, regio, or diastereoselectivity. Recently [2], it has been observed that in the bromination reaction of aromatic substrates, tetraalkylammonium bromide surfactants induce a regioselectivity which depends on the structure of the substrate as well as on that of the surfactant. On the basis of the results observed on the bromination reactions, which have been carried out in the presence of the tribromide salts as precipitates, a few hypothesis have been made on the structure of the precipitates. Here we report the structural determination of two of these surfactants: cetylpyridiniumammonium bromide (CPyB) and cetylquinuclidinium bromide (CQB).

Experimental

Colourless plate-like crystals of cetylpyridiniumammonium bromide were obtained from an aqueous solutions by slow evaporation at room temperature. A crystal of dimension $0.05 \times 0.4 \times 0.5$ mm was mounted on a Nicolet R-3 four-circle diffractometer equipped with graphite monochromatized MoK_α radiation. The unit cell parameters were determined from a least square fit of the angular settings of 14 reflections in the range $30° < 2\theta < 43°$. Intensity data were recorded by the ω-scan technique, with scan rate depending on the intensities. Intensities were corrected for

* Correspondence author (e-mail: ballirano@axrma.uniroma1.it)

Table 1. Crystallographic data and experimental parameters.

Compound	CPyB	CQB
Formula	$C_{21}H_{38}NBr \cdot H_2O$	$C_{23}H_{46}NBr$
M_r	402.461	416.535
Crystal size mm	$0.05 \times 0.4 \times 0.5$	–
Crystal system	triclinic	triclinic
Space group	$P\bar{1}$	$P\bar{1}$
Z	2	2
a, Å	7.618(2)	8.1395(8)
b, Å	5.554(1)	6.4475(7)
c, Å	27.474(7)	25.237(2)
α, deg	95.03(2)	92.921(6)
β, deg	95.65(2)	93.123(9)
γ, deg	100.89(2)	111.956(9)
V, Å^3	1129.2(5)	1222.9(2)
D_{calc}, g · cm^{-3}	1.184	1.130
$F(000)$	432	–
Radiation	MoK_α	CuK_α
λ, Å	0.71073	1.54060
T, K	293	293
Obs. reflections	3672	–
R	0.066	–
wR	0.054	–
R_p	–	0.097
wR_p	–	0.128
R_{exp}	–	0.078
R_{Bragg}	–	0.127

the anisotropy of absorption by means of φ-scan curves obtained for four reflections with $\chi \sim 90°$. Three standard reflections, monitored every 100 reflections showed no significant change. A total of 10014 reflections were collected; out of 4320 independent reflections, measured in the range $2.5° < 2\theta < 56.0°$ (R-merged 0.022), 3672 with $I > 1.5\sigma(I)$ ($h = 0$ to 11, $k = -8$ to 8, $l = -40$ to 39), were used for calculations. The structure was solved by the semiinvariant representation package SIR [3]. The E-map computed with the phase set having the highest figure of merit revealed molecular fragments: the location of all the non-H atoms was completed by Fourier recycling. After isotropic and anisotropic refinement of the heavy atoms by full-matrix least-square procedures, all H atoms were found from successive Fourier difference syntheses and their positional parameters, with isotropic temperature factors deduced from the carrier atoms, were varied in the last cycles of refinement. The function minimized was $(w|F_o| - |F_c|)^2$ where $w = (a + |F_o| + c|F_c|^2)^{-1}$ with a and c equal to $2F_{o\,(min)}$ and $2/F_{o\,(max)}$, respectively. The atomic scattering factors were corrected for anomalous dispersion. The final R and wR were 0.066 and 0.054, respectively. Scattering factors were taken from the International Tables for X-ray Crystallography [4]. All the calculations were carried out on the MV8000/II Data General of the CNR Research Area of Roma using local programs [5]. Crystal data are given in Table 1; final atomic parameters of non-H atoms and displacement parameters are listed in Table 2.

Cetylquinuclidinium bromide (CQB) was prepared by alkylation of 1-azabyciclo(2.2.2) octane with 1-bromohexadecane. However, repeated preparations of CQB always led to crystals of very small dimensions that prevented us from carrying out conventional single crystal structure analysis. Therefore we decided to attempt an *ab-initio* structure determination through powder diffractometry. The X-ray powder data of CQB were collected on a Seifert MZ VI automatic diffractometer operating in the conventional Bragg Brentano geometry, using CuK_α radiation. The pattern was collected in step-scan mode in the 3°–80° 2θ angular range, with a step size of 0.025° and a counting time of 8 seconds. The instrument was equipped with two Soller slits and a diffracted-beam curved-crystal pyrolitic graphite monochromator. The sample was located inside a 0.5 mm cavity of a conventional glass sample-holder.

Table 2. Atomic coordinates and equivalent isotropic displacement parameters with their e.s.d.'s in parentheses. Equivalent isotropic atomic displacement factors: $B_{(Eq.)} = 4/3\sum_{ij}(\beta_{ij}a_ia_j)$. Coefficient of β_{ij} are given as:
$\exp[-(\beta_{11}h^2 + \beta_{22}k^2 + \beta_{33}l^2 + 2\beta_{12}hk + 2\beta_{13}hl + 2\beta_{23}kl)]$.

Atom	x	y	z	$B_{(Eq.)}$
CPyB				
Br	−0.5476(1)	0.2869(1)	0.12025(2)	4.78(1)
N	−0.1174(4)	0.0399(6)	0.1073(1)	3.5(1)
C(1)	−0.0212(7)	0.0964(9)	0.1579(2)	4.2(1)
C(2)	−0.0513(7)	0.3288(8)	0.1845(2)	4.1(1)
C(3)	0.0406(7)	0.3625(9)	0.2373(2)	4.2(1)
C(4)	0.0197(7)	0.5955(9)	0.2671(2)	4.2(1)
C(5)	0.1110(7)	0.6254(9)	0.3196(2)	4.3(2)
C(6)	0.0905(7)	0.8559(9)	0.3503(2)	4.3(1)
C(7)	0.1855(7)	0.8840(8)	0.4026(2)	4.2(1)
C(8)	0.1652(7)	1.1133(9)	0.4339(2)	4.2(1)
C(9)	0.2612(7)	1.1423(8)	0.4857(2)	4.2(1)
C(10)	0.2414(7)	1.3713(9)	0.5172(2)	4.3(1)
C(11)	0.3370(7)	1.3995(9)	0.5691(2)	4.3(2)
C(12)	0.3165(7)	1.6282(9)	0.6007(2)	4.4(2)
C(13)	0.4121(7)	1.6561(9)	0.6522(2)	4.4(2)
C(14)	0.3924(7)	1.8855(9)	0.6843(2)	4.3(1)
C(15)	0.4885(8)	1.914(1)	0.7359(2)	4.9(2)
C(16)	0.469(1)	2.142(1)	0.7671(2)	6.2(2)
C(17)	−0.2427(6)	−0.1647(8)	0.0953(2)	4.5(1)
C(18)	−0.3265(7)	−0.221(1)	0.0483(2)	5.7(2)
C(19)	−0.2849(79)	−0.066(1)	0.0134(2)	5.4(2)
C(20)	−0.1582(7)	0.147(1)	0.0267(2)	5.2(2)
C(21)	−0.0748(6)	0.1975(9)	0.0742(2)	4.5(1)
O	−0.7842(3)	−0.2872(8)	0.0919(2)	6.4(1)
H(1)	−0.718(5)	−0.146(8)	0.099(2)	1(1)
H(2)	−0.709(9)	−0.38(1)	0.098(2)	8(1)
CQB				
Br	0.237(2)	0.913(2)	0.1268(2)	4.6(3)
N	−0.159(4)	0.231(3)	0.1354(5)	12.9(6)
C(1)	−0.149(6)	0.288(4)	0.1939(5)	6.4(3)
C(2)	−0.148(6)	0.514(4)	0.2160(7)	6.4(3)
C(3)	−0.082(6)	0.567(3)	0.2746(6)	6.4(3)
C(4)	−0.006(8)	0.814(3)	0.2937(5)	6.4(3)
C(5)	0.018(7)	0.856(3)	0.3552(5)	6.4(3)
C(6)	0.089(7)	1.109(3)	0.3713(6)	6.4(3)
C(7)	0.149(7)	1.158(4)	0.4305(6)	6.4(3)
C(8)	0.181(7)	1.397(4)	0.4510(6)	6.4(3)
C(9)	0.236(7)	1.444(3)	0.5110(6)	6.4(3)
C(10)	0.308(9)	1.693(3)	0.5287(5)	6.4(3)
C(11)	0.356(7)	1.742(3)	0.5889(5)	6.4(3)
C(12)	0.424(7)	1.994(3)	0.6047(5)	6.4(3)
C(13)	0.416(7)	2.046(4)	0.6641(6)	6.4(3)
C(14)	0.525(7)	2.289(4)	0.6834(6)	6.4(3)
C(15)	0.551(8)	2.336(4)	0.7438(6)	6.4(3)
C(16)	0.599(9)	2.582(4)	0.7608(7)	6.4(3)
C(17)	−0.233(6)	−0.011(3)	0.1237(8)	12.9(6)
C(18)	−0.241(7)	−0.064(4)	0.0623(9)	12.9(6)
C(19)	−0.171(4)	0.142(5)	0.0355(5)	12.9(6)
C(20)	−0.275(5)	0.277(8)	0.0465(8)	12.9(6)
C(21)	−0.273(5)	0.325(7)	0.1076(9)	12.9(6)
C(22)	0.019(3)	0.325(7)	0.1174(10)	12.9(6)
C(23)	0.012(4)	0.268(8)	0.0558(10)	12.9(6)

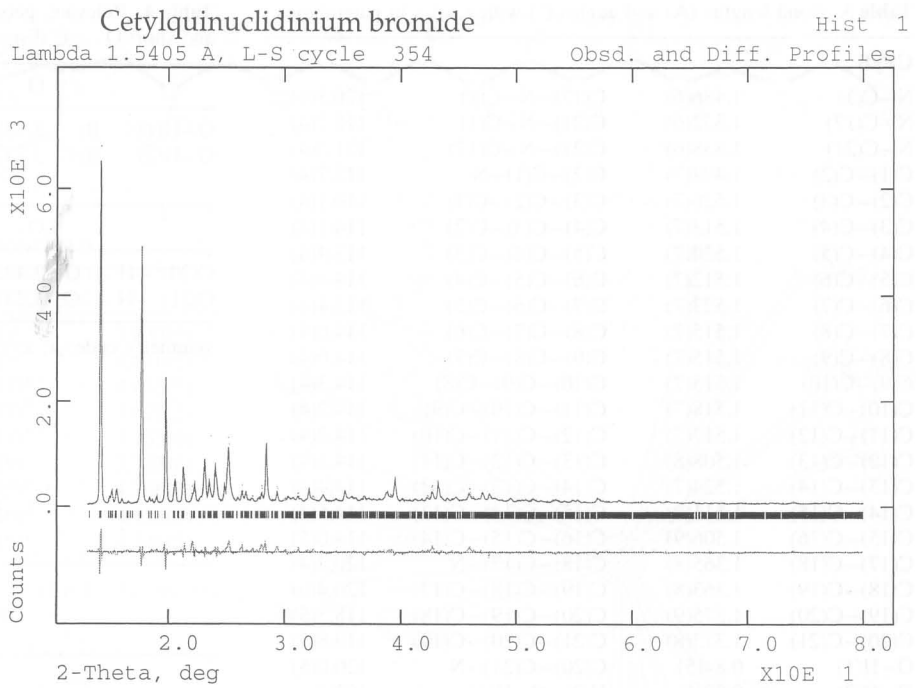

Fig. 1. Experimental (dots) and calculated (continuous line) plots of CQB. The residual intensities are shown at the bottom of the figure. Vertical markers below the experimental/calculated patterns refer to the position of the calculated Bragg reflections.

Starting cell parameters were determined using TREOR [6]: the first 20 peaks, observed through the Seifert peak-search routine and visual inspection of the pattern, were used for the calculation. No solutions were found for cubic, tetragonal, hexagonal/trigonal, orthorhombic, and monoclinic systems. A few possible cells were suggested for the triclinic system: after a careful scrutiny of the various solutions, we observed that only one showed no rejected peaks and a relatively high figure-of-merit. The derived values were $a = 8.09$ Å, $b = 6.43$ Å, $c = 25.14$ Å, $\alpha = 92.8°$, $\beta = 93.1°$, $\gamma = 112.1°$. The *ab-initio* structure determination through Rietveld method was therefore undertaken. The software package we used is the PC version of the well known GSAS (General Structure Analysis System) suite of programs [7]. The power of GSAS is that it allows to use both rigid-body and soft constraints. These options have beneficial effects on the progress of the refinement, greatly reducing the possibility to converge to false minima (for a thorough discussion on restraints and costraints in Rietveld refinement see [8]). In order to build up a suitable structural starting model, a few hypothesis were done: the cetylic group was located inside the unit cell in a position corresponding to that of CPyB. This assumption is supported by the similarities of the two unit cells (see Table 1). As a further starting hypothesis we considered CQB to crystallize in the $P\bar{1}$ space group, the same of CPyB. The starting coordinates of the quinuclidinium group were derived through geometrical calculations. More than a hundred soft-constraints with very high statistical weights were imposed to N–C, C–C bond distances and related angles, in order to perform, at least for the first cycles, a rigid-body refinement. The scattering factor of O was used for methylene moiety. During the first cycles of the refinement only a scale factor, the three terms of the cosine Fourier series describing the background [7], and the cell parameters were allowed to vary. At this stage the difference between calculated and observed intensities was extremely high. The peak-shape was modeled using a multi-term Simpson's rule integration of a pseudo-Voigt function [9]: only the angle-independent Gaussian (GW) and the tan θ-dependent Lorentzian parameter LY were initially refined along with a correction parameter for sample displacement from the focusing circle. The very large misfit between observed and calculated intensity of the (00*l*) reflection was attributed to the presence of some degree of preferred orientation which was modeled through the March-Dollase formalism [10]. Only at this point of the refinement the positional parameters were allowed to vary with a large damping factor. The residuals decreased significantly and the weight of the soft-constraints was gradually reduced. Isotropic displacement parameters were also subsequently refined. The refinement smoothly converged to $R_p = 0.097$, $wR_p = 0.128$, $R_{\text{exp}} = 0.078$, and $R(F^2) = 0.127$. Final atomic coordinates, isotropic displacement parameters are reported in table 2, the observed, calculated, and difference plots in Fig. 1.

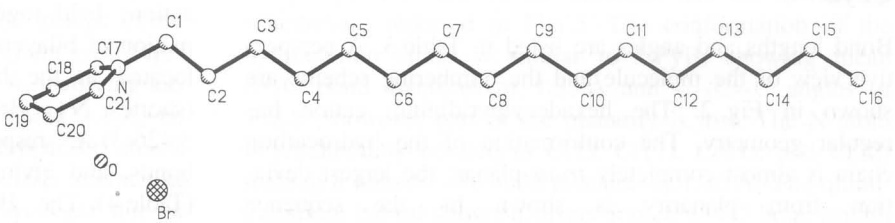

Fig. 2. A view of CPyB showing the atomic numbering scheme. Drawing by SHELXL PC (plus).

Table 3. Bond lengths (Å) and angles (°) with e.s.d.'s in parentheses.

CPyB

N–C(1)	1.486(6)	C(17)–N–C(1)	120.3(4)
N–C(17)	1.332(6)	C(21)–N–C(1)	118.7(4)
N–C(21)	1.338(6)	C(21)–N–C(17)	121.0(4)
C(1)–C(2)	1.494(7)	C(2)–C(1)–N	113.7(4)
C(2)–C(3)	1.526(7)	C(3)–C(2)–C(1)	110.1(4)
C(3)–C(4)	1.513(7)	C(4)–C(3)–C(2)	114.1(4)
C(4)–C(5)	1.520(7)	C(5)–C(4)–C(3)	113.4(4)
C(5)–C(6)	1.512(7)	C(6)–C(5)–C(4)	114.4(4)
C(6)–C(7)	1.523(7)	C(7)–C(6)–C(5)	113.4(4)
C(7)–C(8)	1.515(7)	C(8)–C(7)–C(6)	114.0(4)
C(8)–C(9)	1.515(7)	C(9)–C(8)–C(7)	114.0(4)
C(9)–C(10)	1.515(7)	C(10)–C(9)–C(8)	114.3(4)
C(10)–C(11)	1.518(7)	C(11)–C(10)–C(9)	114.2(4)
C(11)–C(12)	1.517(7)	C(12)–C(11)–C(10)	114.2(4)
C(12)–C(13)	1.508(8)	C(13)–C(12)–C(11)	114.1(4)
C(13)–C(14)	1.524(7)	C(14)–C(13)–C(12)	114.4(4)
C(14)–C(15)	1.511(8)	C(15)–C(14)–C(13)	114.5(4)
C(15)–C(16)	1.506(9)	C(16)–C(15)–C(14)	114.0(5)
C(17)–C(18)	1.365(8)	C(18)–C(17)–N	120.2(4)
C(18)–C(19)	1.363(8)	C(19)–C(18)–C(17)	120.4(6)
C(19)–C(20)	1.375(9)	C(20)–C(19)–C(18)	118.5(5)
C(20)–C(21)	1.373(8)	C(21)–C(20)–C(19)	119.8(5)
O–H(1)	0.84(5)	C(20)–C(21)–N	120.0(5)
O–H(2)	0.87(6)	H(2)–O–H(1)	102(5)

CQB

N–C(1)	1.492(8)	C(1)–N–C(17)	110.4(11)
N–C(17)	1.452(8)	C(1)–N–C(21)	109.7(11)
N–C(21)	1.458(8)	C(1)–N–C(22)	109.1(11)
N–C(22)	1.454(8)	C(17)–N–C(21)	108.5(10)
C(1)–C(2)	1.532(9)	C(17)–N–C(22)	108.3(10)
C(2)–C(3)	1.522(9)	C(21)–N–C(22)	110.8(10)
C(3)–C(4)	1.522(9)	N–C(1)–C(2)	121.4(16)
C(4)–C(5)	1.552(8)	C(1)–C(2)–C(3)	112.5(12)
C(5)–C(6)	1.533(9)	C(2)–C(3)–C(4)	115.4(12)
C(6)–C(7)	1.526(9)	C(3)–C(4)–C(5)	113.3(10)
C(7)–C(8)	1.523(9)	C(4)–C(5)–C(6)	110.2(10)
C(8)–C(9)	1.536(8)	C(5)–C(6)–C(7)	111.4(11)
C(9)–C(10)	1.521(9)	C(6)–C(7)–C(8)	113.2(10)
C(10)–C(11)	1.536(8)	C(7)–C(8)–C(9)	113.0(10)
C(11)–C(12)	1.529(9)	C(8)–C(9)–C(10)	112.6(10)
C(12)–C(13)	1.531(9)	C(9)–C(10)–C(11)	113.3(10)
C(13)–C(14)	1.522(9)	C(10)–C(11)–C(12)	111.2(10)
C(14)–C(15)	1.525(8)	C(11)–C(12)–C(13)	112.5(10)
C(15)–C(16)	1.521(9)	C(12)–C(13)–C(14)	113.3(10)
C(17)–C(18)	1.561(8)	C(13)–C(14)–C(15)	114.8(12)
C(18)–C(19)	1.457(9)	C(14)–C(15)–C(16)	112.4(12)
C(19)–C(20)	1.453(9)	N–C(17)–C(18)	109.1(7)
C(20)–C(21)	1.556(8)	C(17)–C(18)–C(19)	110.4(7)
C(22)–C(23)	1.565(8)	C(18)–C(19)–C(20)	109.1(10)
C(23)–C(19)	1.448(9)	C(18)–C(19)–C(23)	109.3(10)
		C(20)–C(19)–C(23)	108.9(10)
		C(19)–C(20)–C(21)	109.9(7)
		N–C(21)–C(20)	109.7(7)
		N–C(22)–C(23)	110.1(7)
		C(19)–C(23)–C(22)	109.3(7)

Discussion

CPyB

Bond lengths and angles are listed in Table 3. A perspective view of the molecule and the numbering scheme are shown in Fig. 2. The hexadecylpyridinium cation has regular geometry. The conformation of the hydrocarbon chain is almost completely *trans*-planar: the largest deviation from planarity is shown by the sequence

Table 4. Relevant geometric parameters (Å, °) of hydrogen bonds and short O ... C distances for CPyB.

	O ... Br	Br ... H	O–H	O–H ··· Br
O–H(1) ... Br	3.338(5)	2.50(5)	0.84(5)	175(3)
O–H(2) ... Br[a]	3.333(4)	2.48(6)	0.87(6)	169(6)

	O ... C	O ... H	C–H	C–H ... O
C(20)[b]–H ... O	3.422(7)	2.59(6)	1.01(6)	139(4)
C(21)[c]–H ... O	3.237(7)	2.26(5)	1.00(5)	165(3)

symmetry code: a: $x, y-1, z$; b: $-x-1, -y, -z$; c: $x-1, y-1, z$.

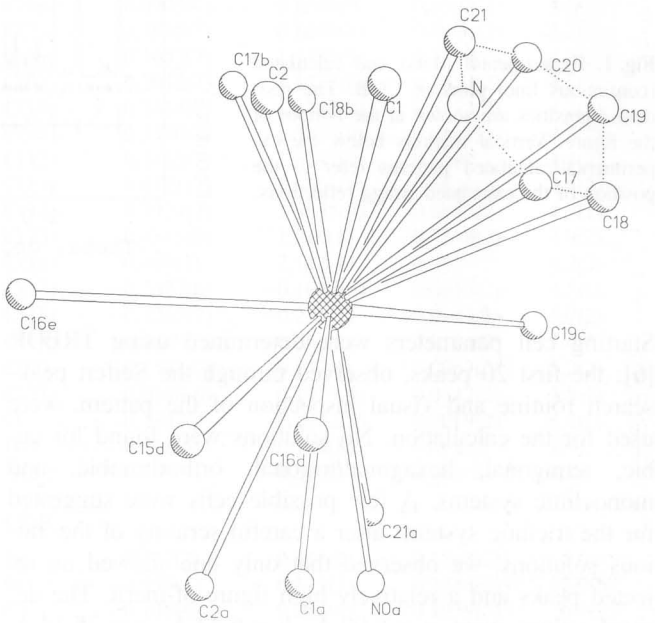

Fig. 3. Coordination of Br^- in CPyB. Dotted lines indicate the location of a complete aromatic ring. Drawing by SHELXL PC (plus).

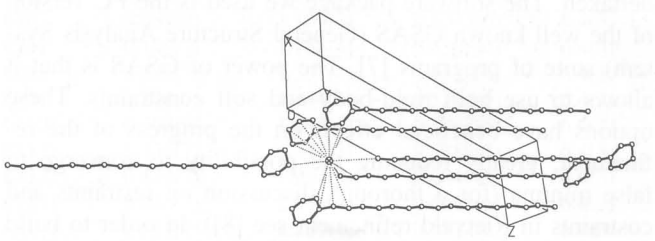

Fig. 4. Molecular packing of CPyB around Br. The unit cell is also shown for clarity. Drawing by SHELXL PC (plus).

N–C(1)–C(2)–C(3) with torsion angle of 175.8(4)°. The torsion angle C(2)–C(1)–N–C(17), giving the orientation of pyridinium ring with respect to the hydrocarbon chain, is −118.4(4)°. The chains lie almost on the *bc* plane with a tilting angle of about 12°. The long hydrocarbon chains are fully interdigitate, giving place to an antiparallel arrangement. Strong Coulomb and van der Waals interactions held together the molecules and cause the formation of bilayers. The Br^- ions and water molecules are located in the hydrocarbon moiety near the N atoms (shortest N ... Br^- and N ... O distances 3.820(3) Å and 3.426(3) Å, respectively), held together by hydrogen bonds, and giving rise to long chains along the *b* axis (Table 4). The Br^- ... O ... Br^- and O ... Br^- ... O an-

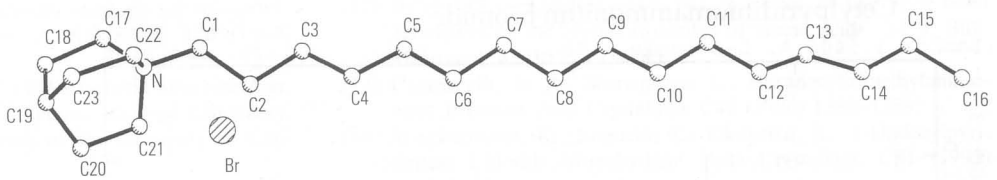

Fig. 5. A view of CQB showing the atomic numbering scheme. Drawing by SHELXL PC (plus).

Table 5. Short contacts (Å) involving Br^- anion.

CPyB			
Br ... N	3.820(3)	Br ... C(1)[a]	3.833(5)
Br ... C(1)	4.387(5)	Br ... C(2)[a]	4.416(5)
Br ... C(2)	3.968(5)	Br ... C(21)[a]	4.015(5)
Br ... C(17)	3.791(4)	Br ... C(17)[b]	3.626(5)
Br ... C(18)	4.021(5)	Br ... C(18)[b]	3.753(6)
Br ... C(19)	4.254(5)	Br ... C(19)[c]	3.783(6)
Br ... C(20)	4.246(4)	Br ... C(15)[d]	4.206(5)
Br ... C(21)	4.035(5)	Br ... C(16)[d]	4.133(5)
Br ... N[a]	4.267(3)	Br ... C(16)[e]	4.146(5)

Symmetry code: a: $x-1, -y, -z$; b: $x, y+1, z$; c: $-x-1, -y, -z$; d: $-x, -y-2, -z+1$; e: $-x, -y-3, -z+1$.

CQB			
Br ... N	4.39(2)	Br ... C(22)[a]	3.72(2)
Br ... C(1)	4.56(2)	Br ... C(23)[a]	3.87(2)
Br ... C(2)	4.10(2)	Br ... N[b]	4.55(2)
Br ... C(21)	4.43(2)	Br ... C(17)[b]	4.16(2)
Br ... C(22)	3.52(2)	Br ... C(18)[b]	4.43(2)
Br ··· C(23)	4.13(2)	Br ··· C(20)[b]	4.45(2)
Br ··· N[a]	4.43(2)	Br ··· C(21)[b]	3.95(2)
Br ··· C(17)[a]	4.03(2)	Br ··· C(19)[c]	4.08(2)
Br ··· C(18)[a]	4.34(2)	Br ··· C(20)[c]	4.54(2)
Br ··· C(19)[a]	4.66(2)	Br ··· C(15)[d]	4.27(2)

Symmetry code: a: $x, y+1, z$; b: $x+1, y+1, z$; c: $-x, -y+1, -z$; d: $-x+1, -y+3, -z+1$.

gles are both 112.7(1)°. The water molecule is also involved in two other short contacts with two carbon atoms and precisely with atoms C(20) and C(21) of the pyridinium ring (Table 4). The existence of such short C–H ... O attractive interactions, which could be described as hydrogen bonds, has been already evidenced [11, 12].

Coulomb interactions involve the bromide ion and the N atoms of the molecules at x, y, z and $x-1, y, z$ with Br^- ... N distances of 3.823(3) Å and 4.267(3) Å respectively, in agreement with the crystal structures of other N-alkyl alides surfactants [13, 14, 15]. The Br^- anion is surrounded by several carbon atoms of the aromatic head and methylenic groups of adiacent molecules (Fig. 3) giving place to an unusual coordination network. The nearest neighbours, within the range 3.6 Å–4.0 Å, are nine carbon atoms: seven of the aromatic ring and two of the methylenic groups adjacent to the ring. Seven other Br^- ... C interactions, within the range 4.1 Å–4.4 Å, involve the atoms C(20) and C(21) of the ring, and the methylenic groups C(1), C(2)[a], C(15)[d] and the methyl groups C(16)[d] and C(16)[e] of the terminal part of the chain (see Fig. 4 and Table 5). Some contacts of about 4.0 Å, involving aromatic C atoms, and C ... C contacts of about 4.1 Å, between methylenic groups of adiacent hydrocarbon chains, contribute to stabilize the bilayer. Attractive interactions between polar regions of face-to-face bilayers are due essentially to the unusual hydrogen bond involving the water molecule and C(21)[b], to the short interaction Br^- ... C(19)[c] and to many C ... C short contacts in the range 3.5 Å–4.0 Å, involving C aromatic atoms.

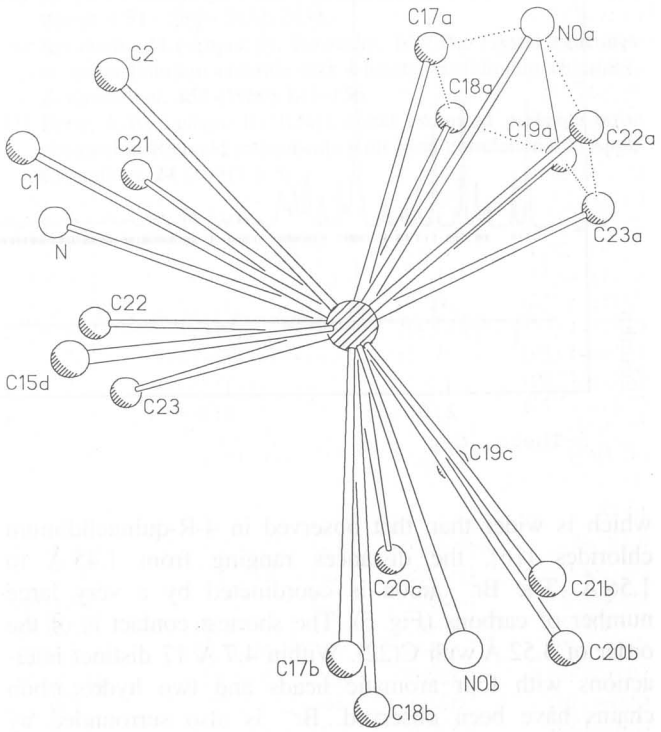

Fig. 6. Coordination of Br^- in CQB. The line connecting N(0)[a] and C(19)[a] marks the edge derived by the intersection of two planes defined by N(0)[a], C(19)[a], C(20)[a], C(21)[a] and N(0)[a], C(19)[a], C(22)[a], C(23)[a] pertaining to the quinuclidinium fragment. Drawing by SHELXL PC (plus).

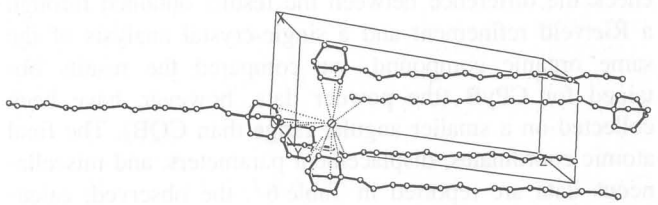

Fig. 7. Molecular packing of CQB around Br^-. The unit cell is also shown for clarity. Drawing by SHELXL PC (plus).

CQB

Bond distances and angles are listed in Table 3, whereas the perspective view of the molecule and the numbering scheme are reported in Fig. 5. The conformation of the hydrocarbon chain is similar to CPyB, showing mean C–C bond distances of 1.53 Å and C–C–C angles of 112.8°, however part of the planarity is lost. The N atom is tetrahedrally bonded to C(1), C(17), C(21), and C(22) making a mean C–N bond distance of 1.46 Å. The quinuclidinium cation shows a dispersion of C–C bond length

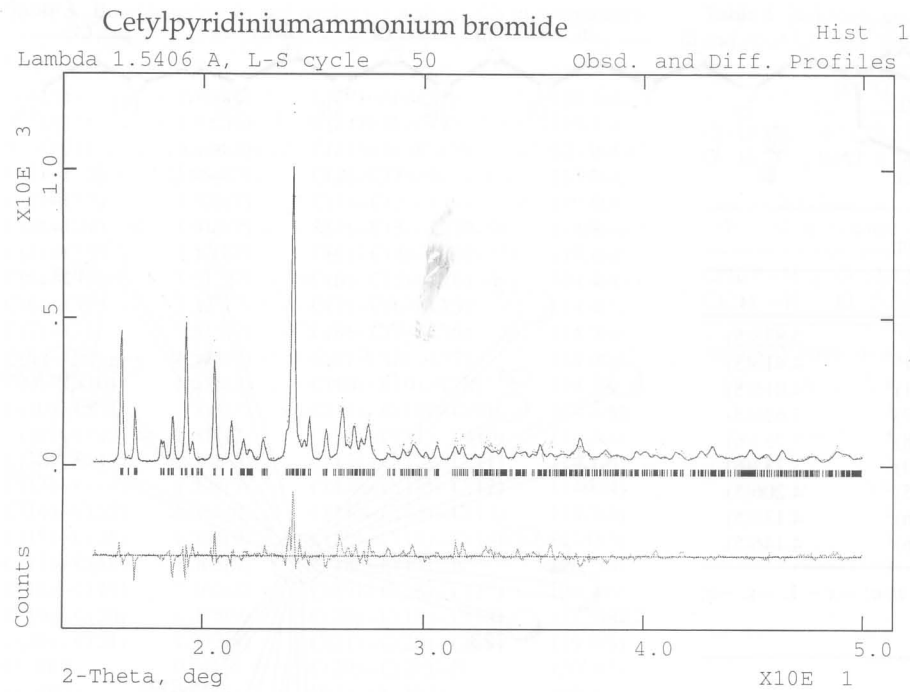

Fig. 8. Experimental (dots), calculated (continuous line), and difference (below) plots of CPyB. Vertical markers at the bottom of the figure refer to the position of the calculated Bragg reflections.

which is wider than that observed in 4-R-quinuclidinium chlorides [16], the distances ranging from 1.45 Å to 1.56 Å. The Br^- anion is coordinated by a very large number of carbons (Fig. 6). The shortest contact is of the order of 3.52 Å with C(22). Within 4.7 Å 17 distinct interactions with four aromatic heads and two hydrocarbon chains have been observed. Br^- is also surrounded by three N atoms with distances in the range of 4.40 Å to 4.55 Å (Fig. 7 and Table 5). As a final remark, however, it must be indicated that all the reported standard deviations of the Rietveld refinement are very optimistic, as pointed out in various papers (see for example [17]). In order to check the difference between the results obtained through a Rietveld refinement and a single-crystal analysis of the same organic compound, we compared the results obtained for CPyB (the powder data, however, have been collected on a smaller angular range than CQB). The final atomic coordinates, displacement parameters, and miscellaneous data are reported in Table 6 [1], the observed, calculated, and difference plots in Fig. 8. The average error in the atomic positions is of the order of 0.012 for the x and y coordinates and 0.002 for the z coordinate that has to be compared with mean E.S.D.'s of 0.005 (for x and y) and 0.0009 (for z). These errors may be attributed to the simplification we used during the Rietveld refinement. In fact we add the electronic scattering contribution of the H atoms to the correspondingly bonded C atoms (i.e. $2\,H + C \Rightarrow O$) without considering the delocalization effect on the centre of gravity of the electronic density of the C atoms due to the H atoms. The loss of planarity of the hydrocarbon chain of CQR may be also possibly attributed to this fact, as well as to the implicit limits of the Rietveld refinement (difficulty to estimate the "real intensity" of the overlapped reflection, difficulty to model the peak shape etc.). However it is worth while to emphasize that through the Rietveld method it has been possible to derive structural information that we were not able to obtain through single-crystal structural analysis.

[1] Table available from the authors upon request.

Conclusions

From the shortest $Br^- \ldots Br^-$ distance (that corresponds to the length of the b cell parameter) and to the average $Br^- \ldots N$ distance it is evident that the structure of CPyB is tighter than that of CQB; this is probably due to the planarity and polarizability of the aromatic ring. This result is in agreement with the hypothesis made on the structure of the surfactants [2], following the observation of a higher regioselectivity in the bromination of anilines carried out in the presence of CPyB relatively to CQB.

Acknowledgments. Thanks are due to Dr. Vincenzo Fares and Claudio Veroli of the Istituto di Chimica dei Materiali (ICMAT) of the CNR Research Area of Roma for the help in X-ray powder data acquisition.

References

[1] Fendler, J. H.; Fendler, E. J.: Catalysis in micellar and macromolecular systems. Academic Press, New York, San Francisco, London 1975.

[2] Cerichelli, G.; Luchetti, L.; Mancini, G.: Surfactant control of the ortho/para ratio in the bromination of anilines. 3. Tetrahedron **52** (1996) 2465–2470.

[3] Altomare, A.; Cascarano, G.; Giacovazzo, C.; Guagliardi, A.; Burla, M. C.; Polidori, G.; Camalli, M.: SIR92 – a program for automatic solution of crystal structures by direct methods. J. Appl. Crystallogr. **27** (1994) 435.

[4] International tables for X-ray Crystallography. Vol. IV. Kynock Press. Birmingham 1974 (present distributor Kluwer Academic Publishers, Dordrecht).

[5] Camalli, M.; Capitani, D.; Cascarano, G.; Cerrini, S.; Giacovazzo, C.; Spagna, R.: (Italian Patent No. 35403 c/86). SIR-CAOS User Guide.

[6] Werner, P. E.: Trial-and-error computer methods for the indexing of unknown powder patterns. Z. Kristallogr. **120** (1964) 375–387.
[7] Larson, A. C.; Von Dreele, R. B.: GSAS General Structure Analysis System. LAUR 86-748, Los Alamos National Laboratory, Copyright, 1985–1994, The Regents of the University of California.
[8] Baerlocher, Ch.: Restraints and constraints in Rietveld refinement. In: *The Rietveld Method* (Ed. R. A. Young), p. 186–196. Oxford University Press 1993.
[9] Howard, C. J.: The approximation of asymmetric neutron powder diffraction peaks by sums of gaussians. J. Appl. Crystallogr. **15** (1982) 615–620.
[10] Dollase, W. A.: Correction of intensities for preferred orientation in powder diffractometry: application of the March model. J. Appl. Crystallogr. **19** (1986) 267–272.
[11] Taylor, R.; Kennard, O.: Crystallographic evidence for the existence of C–H ... O, C–H ... N and C–H ... Cl hydrogen bonds. J. Am. Chem. Soc. **104** (1982) 5063–5070.
[12] Jeffrey, G. A.; Maluszynska, H.: A survey of hydrogen bond geometries in the crystal structures of amino acids. Int. J. Biol. Macromol. **4** (1982) 173–185.
[13] Campanelli, A. R.; Scaramuzza, L.: Hexadecyltrimethylammonium Bromide. Acta Crystallogr. C**42** (1986) 1380–1383.
[14] Vongbupnimit, K.; Noguchi, K.; Okuyama, K.: 1-Dodecylpyridinium Chloride Monohydrate. Acta Crystallogr. C**51** (1995) 1940–1941.
[15] Silver, J.; Marsh, J.: n-Dodecylammonium Chloride. Acta Crystallogr. C**51** (1995) 2432–2434.
[16] Kurahashi, M.; Engel, P.; Nowacky, W.: The crystal structures of quinuclidinium chloride and 4-haloquinuclidinium chlorides. Z. Kristallogr. **152** (1980) 147–156.
[17] Berar, J.-F.; Lelann, P.: E.S.D.'s and estimated probable error obtained in Rietveld refinements with local correlations. J. Appl. Crystallogr. **24** (1991) 1–5.